
Association between monocyte-to-lymphocyte ratio and mortality in patients with acute pancreatitis requiring intensive care unit admission: a retrospective cohort study and predictive model establishment based on machine learning

Received: 22 August 2025

Accepted: 27 January 2026

Published online: 15 February 2026

Cite this article as: Yang J., Dong C., Guo M. *et al.* Association between monocyte-to-lymphocyte ratio and mortality in patients with acute pancreatitis requiring intensive care unit admission: a retrospective cohort study and predictive model establishment based on machine learning. *Sci Rep* (2026). <https://doi.org/10.1038/s41598-026-37791-6>

JunYuan Yang, Caitao Dong, Mengmeng Guo, Jingdi Chen, Handong Zou, Hang Gao, Jing Xu, Yang Liu, Wei Wu & Shuai Yang

We are providing an unedited version of this manuscript to give early access to its findings. Before final publication, the manuscript will undergo further editing. Please note there may be errors present which affect the content, and all legal disclaimers apply.

If this paper is publishing under a Transparent Peer Review model then Peer Review reports will publish with the final article.

Association between monocyte-to-lymphocyte ratio and mortality in patients with acute pancreatitis requiring intensive care unit admission: a retrospective cohort study and predictive model establishment based on machine learning

JunYuan Yang^{1#}, Caitao Dong^{2#}, Mengmeng Guo^{3#}, Jingdi Chen⁴, Handong Zou⁵, Hang Gao⁵, Jing Xu⁵, Yang Liu⁶, Wei Wu^{5*}, Shuai Yang^{7*}

1 Department of Oncology, Renmin Hospital of Wuhan University, Wuhan, Hubei, P.R. China.

2 Department of Urology, Renmin Hospital of Wuhan University, Wuhan, Hubei, P.R. China.

3 The First Clinical College of Wuhan University, Wuhan, Hubei, P.R. China.

4 Department of orthopedics, The Airborne Military Hospital, Wuhan, Hubei, P.R. China.

5 Department of Critical Care Medicine, Renmin Hospital of Wuhan University, Wuhan, Hubei, P.R. China.

6 Department of Critical Care Medicine, Xianfeng county people's hospital, En shi, Hubei, P.R. China.

7 Department of Emergency Intensive Care Unit, Zhuhai People's Hospital (The Affiliated Hospital of Beijing Institute of Technology, Zhuhai Clinical Medical College of Jinan University), Zhuhai, Guangdong, P.R. China.

(#) JunYuan Yang, Dong Caitao and Mengmeng Guo contributed equally.

(*) Corresponding author

Wei Wu: Email: weiwu2012@whu.edu.cn

Shuai Yang: Email: ys5898@126.com

Abstract

The purpose of this study was to evaluate the predictive value of monocyte-to-lymphocyte ratio (MLR) on the short-term (28 days) and long-term (365 days) mortality risk in patients with acute pancreatitis (AP) using multiple statistical and machine learning (ML) models. Studies selected 1,044 eligible AP patients from the MIMIC-IV database and divided them into four groups based on their MLR values ($MLR < 0.32$; $0.32 \leq MLR < 0.57$; $0.57 \leq MLR < 1$; $MLR \geq 1$). Findings revealed that MLR demonstrated a U-shaped relationship with patient mortality risk, with the minimal mortality risk occurring at an MLR of approximately 0.57. Cox regression model analysis showed that after adjusting for multiple parameters, MLR was still significantly associated with the risk of death. Moreover, ML model analysis identified that MLR has potential value in predicting AP patient outcomes. This study suggests that MLR can be used as a potential indicator to assess prognostic risk in critically ill patients with AP to support clinical decision-making.

Keywords: Acute pancreatitis, Monocyte-to-lymphocyte ratio, Machine learning, Predictive models, MIMIC database

Introduction

Acute pancreatitis (AP), which is a common inflammatory disease of the exocrine pancreas, causes severe abdominal pain and multiple organ dysfunction, which can result in pancreatic necrosis, chronic organ failure, and mortality^[1]. Although the mortality rate for AP is only 1–5%, the mortality rate for severe acute pancreatitis (SAP) is close to 20% -30%^[2]. The global incidence of AP is increasing; specifically, it has a global incidence of 30-40 cases per 100,000 people per year and has been demonstrated to be more than twice this rate in some regions, thus contributing to high costs for health care systems^[3]. Currently, there is no specific causal treatment for AP^[4], although some underlying causes such as hypertriglyceridemia and gallstones can be managed.

Although the pathophysiological mechanisms of AP have become better understood in recent years, its prognostic assessment remains challenging^[5]. The inflammatory response and immune dysregulation are important causes of the onset and progression of AP^[6]. Consequently, the search for biomarkers that reflect the inflammatory status and immune function of patients is important for the early identification of high-risk patients and improvements in patient prognosis.

ML techniques are becoming increasingly important in health care and have demonstrated considerable potential for accurately predicting survival rates and disease progression in cancer patients^[7]. To clarify, while ML techniques are increasingly utilized to predict patient outcomes in AP, there are significant deficiencies in the methodology of recently published ML based prognostic models in AP patients^[8], and few systems are specifically designed for routine screening of AP-related risks in the ICU. Thus, this study, based on ML algorithms, aimed to construct multiple prediction models and feature analysis methods for data analysis, identify the primary clinical markers influencing AP patients' prognosis, and provide stronger support for clinical decision-making.

The monocyte-to-lymphocyte ratio (MLR) integrates two key immune pathways: monocytes represent systemic inflammation, while lymphocytes reflect immune competence. MLR has rarely been researched in AP. Given the central role of inflammation and immune dysregulation in AP pathogenesis, we hypothesized that MLR could serve as a novel prognostic biomarker in critically ill AP patients.

We focused specifically on AP patients requiring ICU admission because this subgroup experiences the highest morbidity and mortality, representing a critical population where early and accurate prognostic assessment is most urgently needed to guide intensive care resource allocation and therapeutic strategies.

Methods

Data source

This study utilized data from MIMIC-IV v3.0 (Medical Information Mart for Intensive Care), which is a publicly available critical care database containing deidentified records of 94,458 intensive care unit admissions between 2008 and 2022 (Figure 1). MIMIC-IV is a publicly available critical care database from the United States, containing data from Beth Israel Deaconess Medical Center in Boston. The Institutional Review Board of the BIDMC approved a waiver of the author's informed consent. The author (WW) was permitted to access the database (certificate number 56452808).

Inclusion and exclusion criteria

Inclusion criteria: 1. patients aged over 18 years; and 2. patients diagnosed with AP based on the International Classification of Diseases^[9]. Exclusion criteria: 1. patients who had an ICU stay of fewer than twenty-four hours; 2. absent serum monocytes and lymphocytes in the initial laboratory test; and 3. data only being included from a patient's initial hospitalization in cases where the patient experienced multiple ICU stays. Finally, 1044 individuals who met the criteria were selected for inclusion (Figure 1).

Outcome

This study primarily focused on 28-day all-cause mortality as the main outcome, and 365-day all-cause mortality was regarded as the secondary outcome.

Data extraction

We retrieved data from the MIMIC-IV, including demographic information, vital signs, comorbidities, therapies, laboratory data, scoring systems, and prognostic data during follow-up. All of the hematological parameters were assessed for the first time following patient admission to the ICU. The following formula was used for determining the MLR: serum monocytes (K/ μ L)/serum lymphocytes (K/ μ L).

Statistical analysis

Patients were stratified into four groups based on quartiles of MLR values to explore potential nonlinear associations and ensure balanced group sizes for comparative analysis. The normality of distribution was assessed via Shapiro-Wilk tests supplemented by visual examination of the Q-Q plots. Normally distributed continuous variables are presented as the means \pm standard deviations, whereas nonnormally distributed variables are reported as medians (interquartile ranges). Categorical variables are expressed as counts (percentages). Intergroup comparisons were performed via Mann-Whitney U tests for nonparametric continuous data, chi-square tests for categorical variables, or Fisher's exact tests (when appropriate). A two-tailed p value less than 0.05 was considered to be statistically significant. R software was used for all of the statistical analyses (version 4.4.1).

Kaplan-Meier survival analysis with log-rank tests was used to compare 28-day and 365-day survival rates among the four groups.

To control for potential confounding factors in our survival analysis, we constructed multivariate Cox proportional hazards regression models with progressive covariate adjustments. Model I included only the MLR. Model II was adjusted for age, sex, language, marital status, and race. Subsequently, Model III was adjusted for age, hypertension, myocardial infarction, congestive heart failure, cerebrovascular disease, chronic pulmonary disease, diabetes, renal disease, malignant cancer, liver disease, sepsis, sex, language, marital status, and race.

To investigate potential variations in the associations between the MLR and outcomes across different patient subgroups, as well as to examine possible interaction effects, we conducted stratified analyses by using the following variables: (1) demographic characteristics including sex and age (<60 vs. ≥ 60 years) and (2) comorbidities including hypertension and diabetes mellitus (DM). The findings were graphically presented using forest plots. In addition, restricted cubic spline (RCS) plots with four knots were used to identify potential inflection points to assess the linear or nonlinear relationships between the clinical outcomes and the levels of the MLR as continuous variables. The analysis was also adjusted for various confounding factors, including age, hypertension, myocardial infarction, congestive heart failure, cerebrovascular disease, chronic pulmonary disease, diabetes, renal disease, malignant cancer, liver disease, sepsis, sex, language, marital status, and race. For all of the models, the

median values of the MLR were set as a reference.

Model development

We conducted a LASSO regression cross-validation analysis to select variables. In the development of the machine learning (ML) algorithm, acceptable variables were carefully selected and integrated into the algorithm. The dataset was subsequently partitioned into training and validation subsets at a 7:3 ratio. All ML analyses were conducted using R software (version 4.4.1) within the mlr3 ecosystem (version 0.20.2). The modeling workflow was constructed using the mlr3pipelines package. The Cox proportional hazards survival learner (Coxph), conditional inference tree (ctree), gradient boosting machine (GBM), neural network (NN), survival random forest SRC learner (rsf), and extreme gradient boosting survival learner (xgboost) algorithms. For algorithms requiring hyperparameter tuning (ctree, rsf, xgboost, GBM, NN), we performed a 5-fold cross-validated grid search using the mlr3 tuning package. A predefined parameter space was established for each learner, and the optimal hyperparameter set was selected based on maximizing Harrell's C-index. The final model for each algorithm was then refitted on the entire training set using its respective optimal configuration. The key hyperparameters for the final models were as follows: Ctree: alpha = 0.1, minbucket = 25, Rsf: ntree = 200, mtry = 3, nodesize = 21, Xgboost: eta = 0.08917, max_depth = 1, nrounds = 269, GBM: n.trees = 100, interaction.depth = 1, n.minobsinnode = 5, shrinkage = 0.1, NN: num_nodes = c (5, 5, 5), dropout = 0.2631, weight_decay = 0.1331, learning_rate = 0.07773, batch_size = 32. We optimized hyperparameters using grid search and assessed model robustness via five-fold cross-validation. The ROC curve and its corresponding area under the curve (AUC) were used to determine model performance. Clinical effectiveness was evaluated using decision curve analysis (DCA), and the model's accuracy in forecasting absolute risk was assessed using calibration curves. The Shapley additive explanations (SHAP) method was used to explain the optimal model to understand the impact of individual features on the model predictions (Figure 1).

Results

Baseline characteristics

Data were available from 1044 patients. Table 1 displays the baseline characteristics of the study participants. There were 433 (41.48%) females and 611 (58.52%) males, as well as 665

(63.70%) patients with hypertension, 118 (11.30%) patients with myocardial infarctions, 229 (21.93%) patients with congestive heart failure, 71 (6.8%) patients with peripheral vascular disease, 69 (6.61%) patients with cerebrovascular disease, 227 (21.74%) patients with chronic pulmonary disease, 395 (37.84%) patients with diabetes, 243 (23.28%) patients with renal disease, 79 (7.57%) patients with malignant cancer, 368 (35.25%) patients with liver disease, 12 (1.15%) patients with AIDS, and 606 (58.05%) patients with sepsis.

Patients were divided into the following four groups: Group 1 ($MLR < 0.32$), which consisted of 255 individuals; Group 2 ($0.32 \leq MLR < 0.57$), which consisted of 261 individuals; Group 3 ($0.57 \leq MLR < 1$), which consisted of 243 individuals; and Group 4 ($MLR \geq 1$), which consisted of 285 individuals.

Significant variations were observed across MLR groups in multiple clinical parameters (Table 1). The overall patterns suggested that Group 1 tended to have higher values for mean arterial pressure, oxygen saturation, hematocrit, hemoglobin, albumin, calcium, sodium and initial absolute lymphocyte count, while generally showing lower values for prothrombin time, partial thromboplastin time, international normalized ratio, blood cell count, and initial absolute monocyte count. Additionally, the patterns indicated that Group 2 tended to have a greater bicarbonate level and a lower creatinine level. Group 3 was generally associated with a greater platelet count (max) and potassium level (max), alongside a lower anion gap (max), alkaline phosphatase level, and aspartate aminotransferase level (max). Moreover, Group 4 presented the most pronounced pattern, tending to have a greater respiratory rate; greater white blood cell count, anion gap, BUN, creatinine, glucose, prothrombin time, partial thromboplastin time, alanine aminotransferase, aspartate aminotransferase, alkaline phosphatase, total bilirubin, initial absolute monocyte count, Oxford acute severity of illness score, simplified acute physiology score II and acute physiology score III values; and lower mean arterial pressure, temperature, oxygen saturation, hematocrit, albumin, bicarbonate, calcium, chloride, sodium, and initial absolute lymphocyte count values.

Clinical outcomes

Statistically significant differences in survival distribution among the different MLR groups were observed over time (Table 2). The overall patterns indicated that the highest ICU mortality (10.88%) and hospital mortality (20.70%) were numerically observed in Group 4 (the highest

MLR group), while the lowest rates (3.45% and 4.21%, respectively) were noted in Group 2. Regarding length of stay, Group 4 was associated with the longest median ICU stay (2.88 days) and hospital stay (16.04 days), whereas the shortest median durations were observed in Group 1 (1.95 days and 8.19 days, respectively). Mortality rates across various time points (28-day to 365-day) also showed a consistent pattern, with Group 4 demonstrating numerically higher rates and Group 2 showing numerically lower rates compared to other groups.

Kaplan-Meier (K-M) curves demonstrated a significant overall difference in survival probability among the groups at 28 days (log-rank $p < 0.001$, Figure 2). Visual inspection of the curves suggested that patients in the fourth quartile had the poorest estimated survival. In contrast, no significant overall difference was observed in the 365-day survival rates across the groups (Supplementary Figure 1).

In the RCS analysis, both 28-day all-cause mortality (Figure 3A) and 365-day all-cause mortality (Figure 3B) exhibited a U-shaped relationship between the MLR and mortality risk. This pattern persisted irrespective of whether the covariates were adjusted (Supplementary Figure 2).

Cox regression model

The results of the Cox regression analyses for 28-day all-cause mortality are presented in Table 3. Using Q2 as the reference, the mortality risks in Q1 and Q3 were not significantly different across all models (all $p > 0.05$). In contrast, Q4 was associated with a significantly elevated risk compared to Q2 in the crude model (Model 1, HR: 3.63, 95% CI: 2.01-6.54), and this association remained robust after sequential adjustments for demographic factors (Model 2, HR: 3.03, 95% CI: 1.66-5.52) and comprehensive clinical comorbidities (Model 3, HR: 2.91, 95% CI: 1.59-5.32). Furthermore, a significant positive trend was observed across the quartiles (P for trend < 0.001 in all models), indicating a graded relationship between higher MLR levels and increased 28-day mortality risk.

The associations between MLR quartiles and 365-day all-cause mortality are shown in Table 4. In the fully adjusted model (Model 3), both Q1 (HR: 1.63, 95% CI: 1.04-2.56) and Q3 (HR: 1.63, 95% CI: 1.06-2.52) showed a significantly increased mortality risk compared to Q2. The risk was most pronounced in Q4 (HR: 2.81, 95% CI: 1.89-4.17). This pattern was consistent across all models, with significant positive trends (all p for trend < 0.001), reinforcing a strong,

independent association between elevated MLR and long-term mortality. Notably, the emergence of a significant risk in Q1 at 365 days, which was not observed at 28 days, suggests that the predictive power of MLR may extend to long-term outcomes across a broader range of values.

Subgroup analysis

To evaluate the consistency of the association between MLR and mortality across different patient populations, we conducted subgroup analyses for both 28-day (Figure 4A) and 365-day (Figure 4B) all-cause mortality. The analyses stratified patients by sex (male/female), age (≥ 60 / <60 years), and key comorbidities (hypertension, diabetes, myocardial infarction). The increased mortality risk associated with MLR was consistently observed in all subgroups at both time points (all $P < 0.05$). Importantly, no significant interaction effects were detected (P for interaction > 0.05 for all variables), demonstrating that the association remained robust regardless of these baseline characteristics.

Feature selection

Feature selection was performed using LASSO (Least Absolute Shrinkage and Selection Operator) regression with 28-day all-cause mortality as the outcome variable. LASSO regression was used to screen the relevant features of the training set, and the characteristics of the variable coefficients are shown in Figure 5A. The iterative analysis was performed using a ten fold cross-validation method. The 10 variables that were determined to be closely associated with AP included age, temperature_mean, Spo2_min, hemoglobin_max, partial thromboplastin time (PTT_min), bilirubin_total_min, APSIII, heart_failure, cancer, and MLR (Figure 5B).

Model performance comparisons

A K-M survival curve was constructed after splitting, which compared the survival probabilities of the validation set and the derivation set (Supplementary Figure 3). The derivation set and the validation set did not significantly differ in terms of survival probability, thus indicating that the split was reasonable.

To determine the risk of AP patients in the ICU, we built six machine learning models. In the derivation group (Figure 6A), the AUC of the xgboost model was 0.9151, and that of the rsf model was 0.9381, both of which indicated high prediction accuracy. In the validation group (Figure 6B), the Coxph model demonstrated the highest AUC of 0.8908, whereas the xgboost

model had an AUC of 0.8677, and the rsf model had an AUC of 0.8771, both of which were slightly lower than those of the derived populations; however, they still exhibited good predictive performance. Depending on the AUC values in the derivation groups, the Coxph and rsf models may be optimal, especially in applications that require high prediction accuracy.

Model calibration curves were also constructed, which corresponded to the model's performance in the derivation and validation groups (Figure 7). In both groups, the calibration curves for most of the models were close to the reference line, thus suggesting that the models performed well in predicting risk and that the predicted values were in good agreement with the actual values. In the derived group (Figure 7A), the calibration curves for all of the models were relatively close to the reference line, especially in regions with low prediction risk. This result demonstrated that the model was reliable regarding the training data. In the validation group (Figure 7B), the calibration curve of the model was also close to the reference line, thereby suggesting that the model also demonstrated good generalizability for unseen data. Compared with those of the other models, the calibration curves of the Coxph model in the derived groups and the ctree and Coxph models in the validated groups were closer to the reference line in high-risk regions, thus indicating that the predictions in these regions were more accurate.

The DCA curves of the six ML algorithms on two sets of data (the derivation group and the validation group) are presented in Figure 8. Every model (with the exception of GBM) demonstrated a strong net benefit in terms of clinical application over a broad range of threshold probabilities; additionally, the models exhibiting the largest net benefits were the rsf and xgboost models (Figure 8A), as well as the Coxph and xgboost models (Figure 8B). Therefore, based on the DCA curve, the model with the highest net return within a specific threshold range can be selected.

Figure 9 presents the SHAP summary plots for all models, from which two key observations emerge. First, MLR's importance is not an artifact of a single model but is a robust finding across multiple, independent algorithms. Furthermore, the high importance assigned to MLR by non-linear models like RSF, XGBoos and GBM aligns perfectly with our previous finding of a significant non-linear relationship via RCS plots. It confirms that these models effectively capture the complex, U-shaped association between MLR and mortality that a linear Cox model

may partially mask in its feature importance breakdown. Therefore, the combination of the Cox model's superior overall AUC and the cross-model validated importance of MLR via SHAP, provides a more comprehensive and compelling argument for MLR's role as a key prognostic factor. Finally, based on the results, the optimal model was determined to be Coxph. To facilitate clinical application, a nomogram was developed and is presented in supplementary figure 4.

Discussion

Our research identified significant associations between the MLR and increased 28-day, 365-day, and in-hospital mortality in SAP patients. These associations remained significant across different age groups, sexes, and subgroups (type 2 diabetes, hypertension, myocardial infarction) after adjusting for covariates. This is the first study to investigate the link between prognosis and the MLR in SAP patients.

Among the clinical outcomes, the K-M survival curve revealed that the $MLR \geq 1$ group exhibited the highest mortality. Moreover, the RCS analysis revealed a U-shaped association between the MLR and 28-day mortality in AP patients; additionally, the Cox regression model revealed that a substantially greater risk of death was associated with an $MLR \geq 1$. The correlation between the MLR and mortality risk persisted even after controlling for several variables. In addition, the MLR demonstrated a similar trend in the prediction of 365-day mortality, thus suggesting that it has some potential predictive value for long-term prognosis. ML algorithms revealed that the Coxph and rsf models exhibited the highest AUC values in the validation set. Compared with those of the other models, the ctree and Coxph models in the validated groups were closer to the reference line in high-risk regions, thereby indicating that the predictions in these regions were more accurate. Moreover, the DCA curve revealed that the Coxph and xgboost models demonstrated the greatest net benefits in the validation set. The SHAP method was used to visually interpret the Coxph model, and the APS III score and age were determined to be the most important predictive features; additionally, the MLR also had an impact on the model prediction.

Monocytes and lymphocytes are commonly used indicators of disease inflammation and immune status. Monocyte was significantly higher in survivors in sepsis^[10], And low lymphocyte count serves as an independent marker of progressive inflammation^[11]. However, the prediction performance of monocyte or lymphocyte alone is poor.

Monocyte-lymphocyte ratio (MLR) has shown excellent predictive performance in many diseases. A previous study demonstrated that MLR can provide critical insights into the overall physiological conditions of patients with traumatic brain injury (TBI)^[12]. One study revealed that both the identification of those patients with incident symptomatic TB disease and the prediction of subsequent TB infections may benefit from the utilization of the MLR^[13]. The MLR has also been assessed as a predictor of survival in patients with various malignant diseases^[14,15]. Due to the fact that the MLR has rarely been researched in AP, we investigated the relationship between the MLR and mortality in ICU patients with AP to determine the usefulness of the MLR in predicting ICU AP prognosis.

The MLR is a novel inflammatory biomarker that integrates the effects of both inflammatory markers (monocytes and lymphocytes)^[16]. The MLR has exhibited high predictive and prognostic values in a variety of cancers, including endometrial cancer^[17], renal cell carcinoma^[16], and breast cancer^[18]. High expression of MLR was detected in inflammatory diseases. High MLR expression was associated with mortality in acute respiratory distress syndrome^[19]. In addition, the MLR is often used to evaluate the prognosis of pulmonary TB^[20]. The MLR is a convenient and noninvasive inflammatory biomarker^[21] that provides a more complete representation of the balance between inflammation and immune function. However, few studies have investigated the role of the MLR in predicting the prognosis of AP patients. Therefore, more detailed experiments are needed to investigate the association between the MLR and AP.

We used LASSO regression for feature selection and constructed six models, including Coxph, ctree, GBM, NN, rsf, and xgboost. The SHAP approach was subsequently utilized to evaluate the best model (Coxph) and examine how each feature affected the model predictions. SHAP is a method that is used for interpreting ML model predictions; moreover, it quantifies the contribution of each feature to the model predictions^[22], and we utilized this method to determine the ten most crucial feature variables pertaining to AP mortality. Recently, research based on ML and SHAP has shown that the six most important characteristic variables are important for the short-term assessment of AP^[23]. By using a greater number of biochemical indicators, our study further investigated the important predictors and prediction models for 28-day and 365-day all-cause mortality in AP patients. The results demonstrated that the 10

characteristic variables (apsIII, age, hemoglobin_max, heart_failure, cancer, temperature_mean, PTT_min, SpO2_min, MLR, and bilirubin_total_min) involved in the model that was proposed in this study are equally important for predicting the poor prognosis of AP patients.

Research has indicated that in AP patients, a lower SpO2 is associated with a greater mortality rate^[24]. Moreover, AP may be the first manifestation of pancreatic cancer, and patients with malignant tumors such as pancreatic cancer are more likely to have a poor prognosis^[25]. Additionally, several studies have also suggested that elderly patients with AP are likely to have atypical clinical presentations and poor prognoses, which are mainly due to existing comorbidities^[26,27]. In rats with AP, hypothermia can decrease pancreatic inflammation and increase survival^[28]. In addition, the death rate of SAP patients has been shown to be closely associated with PTT^[29]. These results indicate that the previously mentioned variables are trustworthy predictors of AP mortality rates.

In our research, the U-shaped association that was observed between the MLR and mortality may be closely related to the body's inflammatory response and immunomodulatory mechanisms. Monocytes are a vital part of the innate immune system. And lymphocytes possess strong effector mechanisms^[26]. Inflammation is associated with a low lymphocyte count and function^[27]. A higher MLR indicates a high monocyte count, which aggravates local and systemic inflammatory responses, thereby leading to tissue damage^[25]. And the elevated MLR may be caused by the decrease in the lymphocyte count, making it difficult to effectively eliminate inflammatory factors, thus leading to worsening of the disease^[28].

Unlike previous studies, this study not only focused on 28-day mortality but also explored the predictive value of the MLR for long-term prognosis by using 365-day follow-up data, which further expands the potential application of the MLR in the field of AP. In addition, this study used various ML models to analyze the data. These models outperformed traditional statistical methods in accurately identifying key mortality factors and provided robust support for clinical decision-making. Clinically, the MLR (which is a readily accessible biomarker obtained from routine blood tests) demonstrates high utility for early risk stratification, thereby enabling the rapid identification of high-risk AP patients upon admission. Methodologically, the integration of ML algorithms (such as xgboost, rsf, and NN) can facilitate the development of robust prognostic models and feature analysis frameworks, thus advancing predictive analytics in AP

research. These models underscore the role of the MLR in AP.

Despite the use of rigorous methodologies, several limitations existed in this study. First, the data (which were solely derived from the MIMIC-IV database) may have introduced selection bias, thereby limiting generalizability. Second, we were unable to account for certain confounding factors that are potentially result-altering, such as concurrent infections (beyond the diagnosis of sepsis), disease-specific severity scores (e.g., BISAP, Revised Atlanta Criteria), and detailed medication records (e.g., steroids or immunomodulators), which could influence both patient outcomes and MLR values. Future studies should aim to incorporate these critical variables to enhance the robustness and clinical applicability of the prognostic models. Third, when considering model-specific constraints, the Coxph model assumes that the risk ratio is constant over time, which may not be true in some cases, whereas xgboost has high predictive performance but poor model interpretation. Future studies may consider expanding the data sources, optimizing model construction methods, performing in-depth explorations on the interactions between various characteristics, and validating the findings in more health care institutions and patient groups, in order to improve the reliability and usefulness of the results of this study.

Conclusion

This study demonstrated that the likelihoods of short-term and long-term death in AP patients are substantially connected with the MLR, and this association was observed to be U shaped. A comparison of multiple ML models revealed that the Coxph and rsf models performed well in predicting patient prognosis. Via multidimensional data analysis, the MLR was observed to be strongly correlated with AP severity, especially in the prediction of long-term survival. Therefore, the MLR can be used as a potential indicator to assess the prognostic risk of patients with AP in the ICU.

Table 1 Patient demographics and baseline characteristics.

Variables	Total (n = 1044)	G1 (n = 255)	G2 (n = 261)	G3 (n = 243)	G4 (n = 285)	P
Demographics						
Age, M (Q ₁ , Q ₃)	57.00 (46.00, 68.00)	53.00 (44.00,64.50)	57.00 (44.00,68.00)	57.00 (45.50,67.00)	60.00 (49.00,73.00)	<.001
Gender, n(%)						
Male	611 (58.52)	130 (50.98)	158 (60.54)	145 (59.67)	178 (62.46)	
Female	433 (41.48)	125 (49.02)	103 (39.46)	98 (40.33)	107 (37.54)	
Language, n(%)						0.107
English	955 (91.48)	225 (88.24)	244 (93.49)	227 (93.42)	259 (90.88)	
Other	89 (8.52)	30 (11.76)	17 (6.51)	16 (6.58)	26 (9.12)	
Marital Status, n(%)						0.024
Single	449 (43.01)	107 (41.96)	98 (37.55)	98 (40.33)	146 (51.23)	
Married	102 (9.77)	30 (11.76)	29 (11.11)	25 (10.29)	18 (6.32)	
Widowed	428 (41.00)	105 (41.18)	115 (44.06)	109 (44.86)	99 (34.74)	
Divorced	65 (6.23)	13 (5.10)	19 (7.28)	11 (4.53)	22 (7.72)	
Race, n(%)						<.001
White	647 (61.97)	134 (52.55)	175 (67.05)	156 (64.20)	182 (63.86)	
Black/Africa American	168 (16.09)	62 (24.31)	44 (16.86)	35 (14.40)	27 (9.47)	
Other	229 (21.93)	59 (23.14)	42 (16.09)	52 (21.40)	76 (26.67)	
Vital signs						
MAP Mean, M (Q ₁ , Q ₃)	81.00 (73.00, 91.00)	84.00 (75.00,92.50)	82.00 (72.00,92.00)	80.00 (73.50,88.50)	79.00 (71.00,89.00)	0.003
RR Min, M (Q ₁ , Q ₃)	13.00 (10.00, 15.00)	12.00 (10.00,15.00)	12.00 (10.00,15.00)	13.00 (10.00,16.00)	13.00 (11.00,16.00)	0.015
RR Max, M (Q ₁ , Q ₃)	28.00 (25.00, 33.00)	28.00 (24.00,32.00)	28.00 (24.00,34.00)	28.00 (25.00,33.00)	28.00 (24.00,34.00)	0.737
RR Mean, M (Q ₁ , Q ₃)	19.00 (17.00, 23.00)	19.00 (17.00,23.00)	19.00 (17.00,22.00)	19.00 (17.00,22.50)	20.00 (17.00,23.00)	0.198
Temperature Min, M (Q ₁ , Q ₃)	36.60 (36.40, 36.80)	36.60 (36.30,36.80)	36.60 (36.40,36.80)	36.60 (36.40,36.80)	36.50 (36.30,36.70)	0.010
Temperature Max, M (Q ₁ , Q ₃)	37.30 (37.00, 37.80)	37.20 (36.90,37.90)	37.30 (37.10,37.90)	37.30 (37.00,37.80)	37.20 (37.00,37.70)	0.173
Temperature Mean, M (Q ₁ , Q ₃)	36.90 (36.70, 37.20)	36.90 (36.70,37.25)	36.90 (36.70,37.20)	36.90 (36.70,37.30)	36.90 (36.70,37.10)	0.040
Spo2 Min, M (Q ₁ , Q ₃)	92.00 (90.00, 94.00)	93.00 (90.00,95.00)	92.00 (90.00,94.00)	92.00 (90.00,95.00)	91.00 (89.00,94.00)	0.016
Spo2 Max, M (Q ₁ , Q ₃)	100.00(99.00, 100.00)	100.00 (99.00,100.00)	100.00 (99.00,100.00)	100.00 (99.00,100.00)	100.00(99.00,100.00)	0.047
Spo2 Mean, M (Q ₁ , Q ₃)	97.00 (95.00, 98.00)	97.00 (96.00,98.00)	96.00 (95.00,98.00)	97.00 (95.00,98.00)	96.00 (95.00,98.00)	<.001
Laboratory data						
HCT Min, M (Q ₁ , Q ₃)	29.70 (24.70, 34.80)	30.40 (25.20,35.60)	29.50 (25.20,34.50)	29.40 (24.25,34.40)	29.40 (23.40,34.70)	0.135

Variables	Total (n = 1044)	G1 (n = 255)	G2 (n = 261)	G3 (n = 243)	G4 (n = 285)	P
HCT Max, M (Q ₁ , Q ₃)	33.90 (29.00, 38.90)	35.20 (29.90,39.65)	33.30 (29.20,38.10)	34.00 (28.80,38.95)	33.00 (28.00,38.60)	0.028
Hb Min, M (Q ₁ , Q ₃)	9.70 (7.90, 11.50)	10.00 (8.30,11.90)	9.70 (8.10,11.50)	9.40 (7.75,11.25)	9.60 (7.70,11.20)	0.048
Hb Max, M (Q ₁ , Q ₃)	11.00 (9.30, 12.80)	11.50 (9.50,13.30)	10.90 (9.40,12.70)	11.10 (9.30,12.80)	10.70 (9.00,12.50)	0.027
Platelets Min, M (Q ₁ , Q ₃)	163.50(106.75, 244.00)	162.00 (100.00,235.00)	160.00 (106.00,243.00)	166.00 (114.00,259.00)	164.00 (110.00,235.00)	0.508
Platelets Max, M (Q ₁ , Q ₃)	205.00(141.00, 301.25)	202.00 (134.00,287.00)	203.00 (139.00,299.00)	215.00 (142.00,319.00)	206.00 (149.00,282.00)	0.462
Wbc Min, M (Q ₁ , Q ₃)	10.20 (6.60, 14.72)	8.70 (5.95,13.15)	8.90 (5.80,12.20)	10.30 (6.70,14.85)	12.00 (8.50,17.40)	<.001
Wbc Max, M (Q ₁ , Q ₃)	13.65 (9.70, 19.62)	11.80 (8.20,18.10)	12.20 (8.60,16.80)	13.70 (9.85,19.65)	15.80 (11.80,22.30)	<.001
Albumin Min, M (Q ₁ , Q ₃)	3.00 (2.60, 3.42)	3.10 (2.60,3.70)	3.00 (2.70,3.50)	2.90 (2.50,3.40)	2.80 (2.60,3.20)	<.001
Albumin Max, M (Q ₁ , Q ₃)	3.20 (2.80, 3.60)	3.30 (2.90,3.80)	3.20 (2.80,3.60)	3.10 (2.70,3.60)	3.00 (2.70,3.50)	<.001
AG Max, M (Q ₁ , Q ₃)	17.00 (14.00, 21.00)	17.00 (14.00,22.00)	17.00 (14.00,20.00)	16.00 (14.00,20.00)	18.00 (14.00,22.00)	0.118
AG Min, M (Q ₁ , Q ₃)	13.00 (11.00, 15.00)	13.00 (11.00,15.00)	13.00 (10.00,15.00)	13.00 (10.00,15.00)	13.00 (11.00,16.00)	0.043
Bicarbonate Min, M (Q ₁ , Q ₃), mmol/L	20.00 (16.00, 23.00)	20.00 (16.00,23.00)	21.00 (17.00,23.00)	20.00 (17.00,23.00)	19.00 (16.00,23.00)	0.102
Bicarbonate Max, M (Q ₁ , Q ₃), mmol/L	23.00 (20.00, 26.00)	23.00 (20.00,26.00)	23.00 (21.00,26.00)	23.00 (21.00,25.50)	23.00 (19.00,25.00)	0.115
Bun Min, M (Q ₁ , Q ₃), mg/dL	16.00 (9.00, 28.00)	14.00 (8.00,23.00)	14.00 (9.00,21.00)	16.00 (9.00,32.00)	20.00 (12.00,36.00)	<.001
Bun Max, M (Q ₁ , Q ₃), mg/dL	20.00 (12.00, 37.00)	18.00 (12.00,32.50)	18.00 (12.00,28.00)	21.00 (11.50,42.00)	25.00 (15.00,46.00)	<.001
Calcium Min, M (Q ₁ , Q ₃), mg/dL	7.90 (7.30, 8.40)	8.00 (7.40,8.40)	7.90 (7.30,8.40)	8.00 (7.40,8.50)	7.80 (7.20,8.30)	0.059
Calcium Max, M (Q ₁ , Q ₃), mg/dL	8.40 (7.90, 8.90)	8.60 (8.15,9.00)	8.40 (8.00,8.90)	8.50 (7.95,9.00)	8.30 (7.70,8.80)	<.001
Chloride Min, M (Q ₁ , Q ₃), mEq/L	100.00(96.00, 104.00)	100.00 (95.00,104.00)	101.00 (97.00,105.00)	100.00 (96.00,105.00)	99.00 (94.00,104.00)	0.120
Chloride Max, M (Q ₁ , Q ₃), mEq/L	105.00(100.75, 109.00)	105.00 (102.00,110.00)	105.00 (101.00,109.00)	104.00 (100.00,109.00)	103.00 (99.00,108.00)	<.001
Creatinine Min, M (Q ₁ , Q ₃), mg/dL	0.90 (0.60, 1.50)	0.80 (0.60,1.40)	0.80 (0.60,1.30)	0.90 (0.60,1.70)	1.00 (0.70,2.20)	<.001
Creatinine Max, M (Q ₁ , Q ₃), mg/dL	1.10 (0.80, 2.12)	1.10 (0.80,1.85)	1.00 (0.70,1.80)	1.10 (0.80,2.15)	1.40 (0.80,2.80)	<.001
Glucose Min, M (Q ₁ , Q ₃), g/dL	111.00(91.00, 137.00)	108.00 (88.50,136.50)	110.00 (89.00,134.00)	112.00 (91.00,139.00)	113.00(94.00,138.00)	0.577
Glucose Max, M (Q ₁ , Q ₃), g/dL	157.00(121.00, 225.25)	163.00 (121.50,263.50)	152.00 (121.00,212.00)	156.00(119.50,212.50)	155.00(125.00,208.00)	0.229

Variables	Total (n = 1044)	G1 (n = 255)	G2 (n = 261)	G3 (n = 243)	G4 (n = 285)	P
Sodium Min, M (Q ₁ , Q ₃), mEq/L,	136.00(132.0, 0, 138.00)	136.00 (132.00,139.00)	136.00 (133.00,139.00)	136.00 (132.00,138.00)	135.00 (131.00,138.00)	0.065
Sodium Max, M (Q ₁ , Q ₃), mEq/L,	139.00(136.0, 0, 142.00)	140.00 (137.00,143.00)	139.00 (137.00,142.00)	139.00 (136.00,142.00)	138.00 (135.00,141.00)	0.002
Potassium Min, M (Q ₁ , Q ₃), mEq/L	3.80 (3.40, 4.10)	3.70 (3.40,4.10)	3.80 (3.50,4.10)	3.80 (3.40,4.10)	3.80 (3.40,4.20)	0.574
Potassium Max, M (Q ₁ , Q ₃), mEq/L,	4.40 (4.00, 5.10)	4.40 (4.00,5.10)	4.40 (4.10,4.90)	4.50 (4.10,5.10)	4.40 (4.00,5.20)	0.603
Inr Min, M (Q ₁ , Q ₃)	1.30 (1.10, 1.50)	1.20 (1.10,1.40)	1.30 (1.10,1.50)	1.30 (1.10,1.50)	1.30 (1.20,1.70)	<.001
Inr Max, M (Q ₁ , Q ₃)	1.40 (1.20, 1.70)	1.30 (1.20,1.60)	1.40 (1.20,1.70)	1.40 (1.20,1.70)	1.40 (1.20,1.90)	0.015
Pt Min, M (Q ₁ , Q ₃), s	14.10 (12.40, 16.40)	13.30 (12.10,15.55)	14.00 (12.50,16.10)	14.20 (12.35,16.25)	14.60 (12.80,18.10)	<.001
Pt Max, M (Q ₁ , Q ₃), s	15.10 (13.10, 19.00)	14.80 (12.70,17.90)	15.00 (13.10,18.50)	15.20 (13.15,18.60)	15.60 (13.60,21.30)	0.013
Ptt Min, M (Q ₁ , Q ₃), s	30.20 (26.70, 34.30)	29.80 (26.60,33.75)	30.00 (26.80,34.20)	29.80 (26.70,33.65)	30.90 (26.80,36.30)	0.117
Ptt Max, M (Q ₁ , Q ₃), s	33.80 (28.60, 42.90)	32.50 (28.35,44.75)	32.80 (28.50,40.70)	33.70 (28.45,42.85)	34.90 (29.50,44.50)	0.122
Alt Min, M (Q ₁ , Q ₃), U/L	41.00 (20.00, 109.25)	41.00 (19.50,105.00)	42.00 (19.00,126.00)	31.00 (17.50,77.50)	51.00 (25.00,127.00)	0.001
Alt Max, M (Q ₁ , Q ₃),U/L,	48.50 (23.00, 147.25)	48.00 (24.50,140.00)	49.00 (22.00,183.00)	36.00 (20.00,98.00)	60.00 (29.00,167.00)	0.001
Alp Min, M (Q ₁ , Q ₃), U/L	112.00(72.00, 188.00)	114.00 (74.00,188.00)	112.00 (70.00,175.00)	101.00 (69.00,177.00)	119.00 (74.00,205.00)	0.176
Alp Max, M (Q ₁ , Q ₃), U/L	127.00(80.00, 219.25)	136.00 (86.00,215.50)	124.00 (78.00,216.00)	111.00 (77.50,203.50)	136.00 (81.00,238.00)	0.114
Ast Min, M (Q ₁ , Q ₃),U/L,	61.00 (28.00, 142.00)	65.00 (27.50,156.00)	50.00 (27.00,140.00)	50.00 (23.00,102.00)	84.00 (35.00,159.00)	<.001
Ast Max, M (Q ₁ , Q ₃), U/L	80.00 (34.00, 203.25)	81.00 (35.00,205.00)	72.00 (32.00,216.00)	59.00 (29.50,149.50)	108.00 (42.00,234.00)	<.001
Bilirubin Total Min, M (Q ₁ , Q ₃)	1.00 (0.50, 2.50)	0.80 (0.40,2.00)	0.90 (0.50,2.30)	0.80 (0.40,2.30)	1.60 (0.60,4.10)	<.001
Bilirubin Total Max, M (Q ₁ , Q ₃)	1.20 (0.60, 3.40)	1.00 (0.50,2.70)	1.20 (0.50,3.10)	1.00 (0.50,3.25)	2.00 (0.80,5.20)	<.001
First Monocytes Abs, M (Q ₁ , Q ₃), K/ μ L	0.69 (0.45, 1.07)	0.43 (0.25,0.60)	0.59 (0.42,0.80)	0.84 (0.58,1.18)	1.08 (0.78,1.49)	<.001
First Lymphocytes Abs, M (Q ₁ , Q ₃), K/ μ L	1.19 (0.71, 1.86)	1.93 (1.16,2.84)	1.40 (0.99,1.97)	1.16 (0.80,1.60)	0.67 (0.47,0.98)	<.001
Scoring system						
CCI, M (Q ₁ , Q ₃)	5.00 (3.00, 7.00)	4.00 (2.00,6.00)	4.00 (3.00,6.00)	5.00 (3.00,7.00)	5.00 (3.00,7.00)	<.001
Apsiii, M (Q ₁ , Q ₃)	48.00 (36.00, 68.00)	45.00 (34.00,68.00)	43.00 (33.00,61.00)	49.00 (37.00,64.50)	55.00 (40.00,78.00)	<.001
Sapsii, M (Q ₁ , Q ₃)	32.00 (23.00, 44.00)	29.00 (20.00,41.50)	29.00 (21.00,41.00)	34.00 (24.00,44.00)	37.00 (28.00,49.00)	<.001

Variables	Total (n = 1044)	G1 (n = 255)	G2 (n = 261)	G3 (n = 243)	G4 (n = 285)	P
Oasis, M (Q ₁ , Q ₃)	31.00 (25.00, 39.00)	29.00 (23.00,39.00)	30.00 (24.00,38.00)	32.00 (25.50,38.00)	34.00 (28.00,40.00)	<.001
Comorbidities,n(%)						
Hypertension, n(%)						0.039
survival	379 (36.30)	93 (36.47)	113 (43.30)	79 (32.51)	94 (32.98)	
death	665 (63.70)	162 (63.53)	148 (56.70)	164 (67.49)	191 (67.02)	
Myocardial Infarct, n(%)						0.335
survival	926 (88.70)	223 (87.45)	239 (91.57)	211 (86.83)	253 (88.77)	
death	118 (11.30)	32 (12.55)	22 (8.43)	32 (13.17)	32 (11.23)	
Congestive Heart Failure, n(%)						0.114
survival	815 (78.07)	213 (83.53)	200 (76.63)	186 (76.54)	216 (75.79)	
death	229 (21.93)	42 (16.47)	61 (23.37)	57 (23.46)	69 (24.21)	
Peripheral Vascular Disease, n(%)						0.384
survival	973 (93.20)	241 (94.51)	247 (94.64)	223 (91.77)	262 (91.93)	
death	71 (6.80)	14 (5.49)	14 (5.36)	20 (8.23)	23 (8.07)	
Cerebrovascular Disease, n(%)						0.197
survival	975 (93.39)	234 (91.76)	251 (96.17)	225 (92.59)	265 (92.98)	
death	69 (6.61)	21 (8.24)	10 (3.83)	18 (7.41)	20 (7.02)	
Chronic Pulmonary Disease, n(%)						0.263
survival	817 (78.26)	198 (77.65)	194 (74.33)	195 (80.25)	230 (80.70)	
death	227 (21.74)	57 (22.35)	67 (25.67)	48 (19.75)	55 (19.30)	
Diabetes, n(%)						0.052
survival	649 (62.16)	140 (54.90)	168 (64.37)	159 (65.43)	182 (63.86)	
death	395 (37.84)	115 (45.10)	93 (35.63)	84 (34.57)	103 (36.14)	
Renal Disease, n(%)						0.002
survival	801 (76.72)	212 (83.14)	208 (79.69)	182 (74.90)	199 (69.82)	
death	243 (23.28)	43 (16.86)	53 (20.31)	61 (25.10)	86 (30.18)	
Malignant Cancer, n(%)						0.508
survival	965 (92.43)	237 (92.94)	246 (94.25)	222 (91.36)	260 (91.23)	
death	79 (7.57)	18 (7.06)	15 (5.75)	21 (8.64)	25 (8.77)	
Liver Disease, n(%)						0.342
survival	676 (64.75)	171 (67.06)	174 (66.67)	146 (60.08)	185 (64.91)	
death	368 (35.25)	84 (32.94)	87 (33.33)	97 (39.92)	100 (35.09)	
Aids, n(%)						0.475
survival	1032 (98.85)	250 (98.04)	258 (98.85)	242 (99.59)	282 (98.95)	
death	12 (1.15)	5 (1.96)	3 (1.15)	1 (0.41)	3 (1.05)	
Sepsis, n(%)						<.001
survival	438 (41.95)	143 (56.08)	110 (42.15)	93 (38.27)	92 (32.28)	
death	606 (58.05)	112 (43.92)	151 (57.85)	150 (61.73)	193 (67.72)	
Therapies, n (%)						

Variables	Total (n = 1044)	G1 (n = 255)	G2 (n = 261)	G3 (n = 243)	G4 (n = 285)	P
CRRT, n(%)						0.009
No	928 (88.89)	232 (90.98)	237 (90.80)	221 (90.95)	238 (83.51)	
Yes	116 (11.11)	23 (9.02)	24 (9.20)	22 (9.05)	47 (16.49)	
Norepinephrine, n(%)						0.007
No	786 (75.29)	202 (79.22)	208 (79.69)	181 (74.49)	195 (68.42)	
Yes	258 (24.71)	53 (20.78)	53 (20.31)	62 (25.51)	90 (31.58)	
Dobutamine, n(%)						0.105
No	1031 (98.75)	251 (98.43)	260 (99.62)	242 (99.59)	278 (97.54)	
Yes	13 (1.25)	4 (1.57)	1 (0.38)	1 (0.41)	7 (2.46)	
Dopamine, n(%)						0.383
No	1026 (98.28)	253 (99.22)	254 (97.32)	238 (97.94)	281 (98.60)	
Yes	18 (1.72)	2 (0.78)	7 (2.68)	5 (2.06)	4 (1.40)	
Vasopressin, n(%)						0.010
No	921 (88.22)	228 (89.41)	237 (90.80)	220 (90.53)	236 (82.81)	
Yes	123 (11.78)	27 (10.59)	24 (9.20)	23 (9.47)	49 (17.19)	
Epinephrine, n(%)						0.030
No	1010 (96.74)	242 (94.90)	256 (98.08)	240 (98.77)	272 (95.44)	
Yes	34 (3.26)	13 (5.10)	5 (1.92)	3 (1.23)	13 (4.56)	

Group 1: MLR<0.32; Group 2: 0.32≤MLR<0.57; Group 3: 0.57≤MLR<1; Group 4: MLR≥1

M: Median, Q₁: 1st Quartile, Q₃: 3st Quartile

MAP, mean arterial pressure ; RR, respiratory rate ; SPO₂, oxygen saturation ; Hct, Hematocrit ; Hb, Hemoglobin ;

WBC, White Blood Cell ; AG, Anion gap ; PT, prothrombin time ; PTT, partial thromboplastin time ;

INR, international normalized ratio ; ALT, alanine aminotransferase ; AST, aspartate aminotransferase ;

ALP, alkaline phosphatase; CRRT, Continuous Renal Replacement Therapy; Los, Length of Stay; Abs, Absolute;

MLR, monocyte to lymphocyte ratio ; CCI, Charlson Comorbidity Index ; OASISO, Oxford acute severity of illness score ;

SAPS II, Simplified Acute Physiology Score II ; APS III, Acute physiology score III.

Table 2. Clinical outcomes

Variables	Total (n = 1044)	G1 (n = 255)	G2 (n = 261)	G3 (n = 243)	G4 (n = 285)	P
Status 28, n(%)						<.001
survival	936 (89.66)	234 (91.76)	247 (94.64)	222 (91.36)	233 (81.75)	
death	108 (10.34)	21 (8.24)	14 (5.36)	21 (8.64)	52 (18.25)	
Status 60, n(%)						<.001
survival	893 (85.54)	227 (89.02)	243 (93.10)	206 (84.77)	217 (76.14)	
death	151 (14.46)	28 (10.98)	18 (6.90)	37 (15.23)	68 (23.86)	
Status 90, n(%)						<.001
survival	868 (83.14)	222 (87.06)	238 (91.19)	202 (83.13)	206 (72.28)	
death	176 (16.86)	33 (12.94)	23 (8.81)	41 (16.87)	79 (27.72)	
Status 180, n(%)						<.001
survival	841 (80.56)	220 (86.27)	236 (90.42)	194 (79.84)	191 (67.02)	
death	203 (19.44)	35 (13.73)	25 (9.58)	49 (20.16)	94 (32.98)	
Status 365, n(%)						<.001
survival	803 (76.92)	208 (81.57)	227 (86.97)	188 (77.37)	180 (63.16)	
death	241 (23.08)	47 (18.43)	34 (13.03)	55 (22.63)	105 (36.84)	
Icu Death, n(%)						<.001
survival	982 (94.06)	241 (94.51)	252 (96.55)	235 (96.71)	254 (89.12)	
death	62 (5.94)	14 (5.49)	9 (3.45)	8 (3.29)	31 (10.88)	
Hospital Expire Flag, n(%)						<.001
survival	933 (89.37)	237 (92.94)	250 (95.79)	220 (90.53)	226 (79.30)	
death	111 (10.63)	18 (7.06)	11 (4.21)	23 (9.47)	59 (20.70)	
Los Icu, M (Q ₁ , Q ₃)	2.33 (1.27, 5.67)	1.95 (1.16,4.39)	2.23 (1.26,5.17)	2.54 (1.29,5.67)	2.88 (1.39,6.96)	0.010
Los Hospital, M (Q ₁ , Q ₃)	11.85 (5.86, 22.56)	8.19 (4.78,19.45)	8.97 (4.85,19.68)	12.52 (6.52,26.01)	16.04 (8.37,28.79)	<.001

Group 1: MLR<0.32; Group 2: 0.32≤MLR<0.57; Group 3: 0.57≤MLR<1; Group 4: MLR≥1

M: Median, Q₁: 1st Quartile, Q₃: 3st Quartile.

Table 3 Cox regression model (28-day all-cause mortality)

Variables	Model1		Model2		Model3	
	HR (95%CI)	P	HR (95%CI)	P	HR (95%CI)	P
MLR 4 group						
Quartile 1	1.57 (0.80 ~ 3.08)	0.194	1.58 (0.80 ~ 3.14)	0.189	1.79 (0.90 ~ 3.56)	0.095
Quartile 2	1.00 (Reference)		1.00 (Reference)		1.00 (Reference)	
Quartile 3	1.64 (0.83 ~ 3.22)	0.154	1.54 (0.78 ~ 3.04)	0.210	1.39 (0.70 ~ 2.76)	0.346
Quartile 4	3.63 (2.01 ~ 6.54)	<.001	3.03 (1.66 ~ 5.52)	<.001	2.91 (1.59 ~ 5.32)	<.001
HR for trend	2.53 (1.72 ~ 3.70)		2.15 (1.44 ~ 3.19)		2.00 (1.34 ~ 2.99)	
P for trend		<.001		<.001		<.001

Quartile 1 (MLR < 0.32) ; Quartile 2: 0.32≤MLR < 0.57; Quartile 3: 0.57≤MLR < 1; Quartile 4: MLR≥1

HR: Hazard Ratio, CI: Confidence Interval

Model 1: Crude

Model 2: Adjust: age, gender, language, marital status, race

Model 3: Adjust: age, hypertension, myocardial infarct, congestive heart failure, cerebrovascular disease, chronic pulmonary disease, diabetes, renal disease, malignant cancer, liver disease, sepsis, gender, language, marital status, race

Table 4. Cox regression model (365-day all-cause mortality)

Variables	Model1		Model2		Model3	
	HR (95%CI)	P	HR (95%CI)	P	HR (95%CI)	P
MLR 4 group						
Quartile 1	1.46 (0.94 ~ 2.28)	0.090	1.55 (0.99 ~ 2.42)	0.055	1.63 (1.04 ~ 2.56)	0.032
Quartile 2	1.00 (Reference)		1.00 (Reference)		1.00 (Reference)	
Quartile 3	1.84 (1.20 ~ 2.83)	0.005	1.82 (1.18 ~ 2.79)	0.006	1.63 (1.06 ~ 2.52)	0.027
Quartile 4	3.33 (2.26 ~ 4.90)	<.001	2.90 (1.96 ~ 4.29)	<.001	2.81 (1.89 ~ 4.17)	<.001
HR for trend	2.36 (1.83 ~ 3.05)		2.03 (1.56 ~ 2.65)		1.96 (1.50 ~ 2.58)	
P for trend		<.001		<.001		<.001

Quartile 1 (MLR < 0.32) ; Quartile 2: 0.32≤MLR < 0.57; Quartile 3: 0.57≤MLR < 1; Quartile 4: MLR≥1

HR: Hazard Ratio, CI: Confidence Interval

Model1: Crude

Model2: Adjust: age, gender, language, marital status, race

Model3: Adjust: age, hypertension, myocardial infarct, congestive heart failure, cerebrovascular disease, chronic pulmonary disease, diabetes, renal disease, malignant cancer, liver disease, sepsis, gender, language, marital status, race

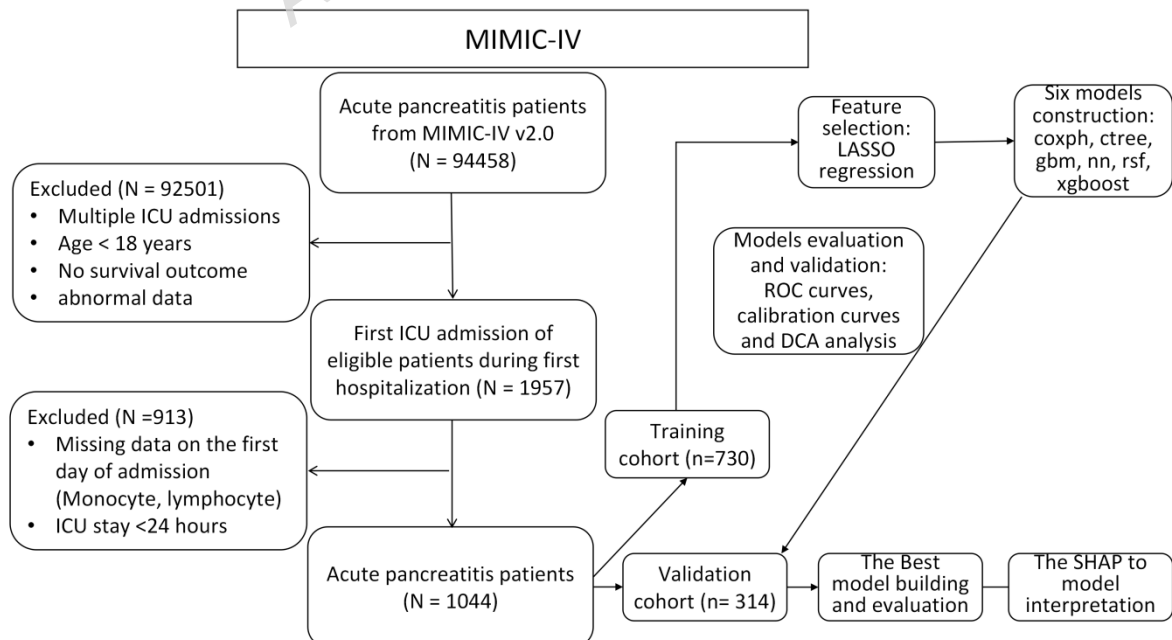
Fig1. Screening process for AP patients in ICU and the research process.

Fig 2.28-day KM survival curve. KM curves showing the survival rates at 28 days for each quartile. MLR: Quartile 1 (<0.32), Quartile 2 ($0.32 \leq \text{MLR} < 0.57$), Quartile 3 ($0.57 \leq \text{MLR} < 1$), and Quartile 4 ($\text{MLR} \geq 1$).

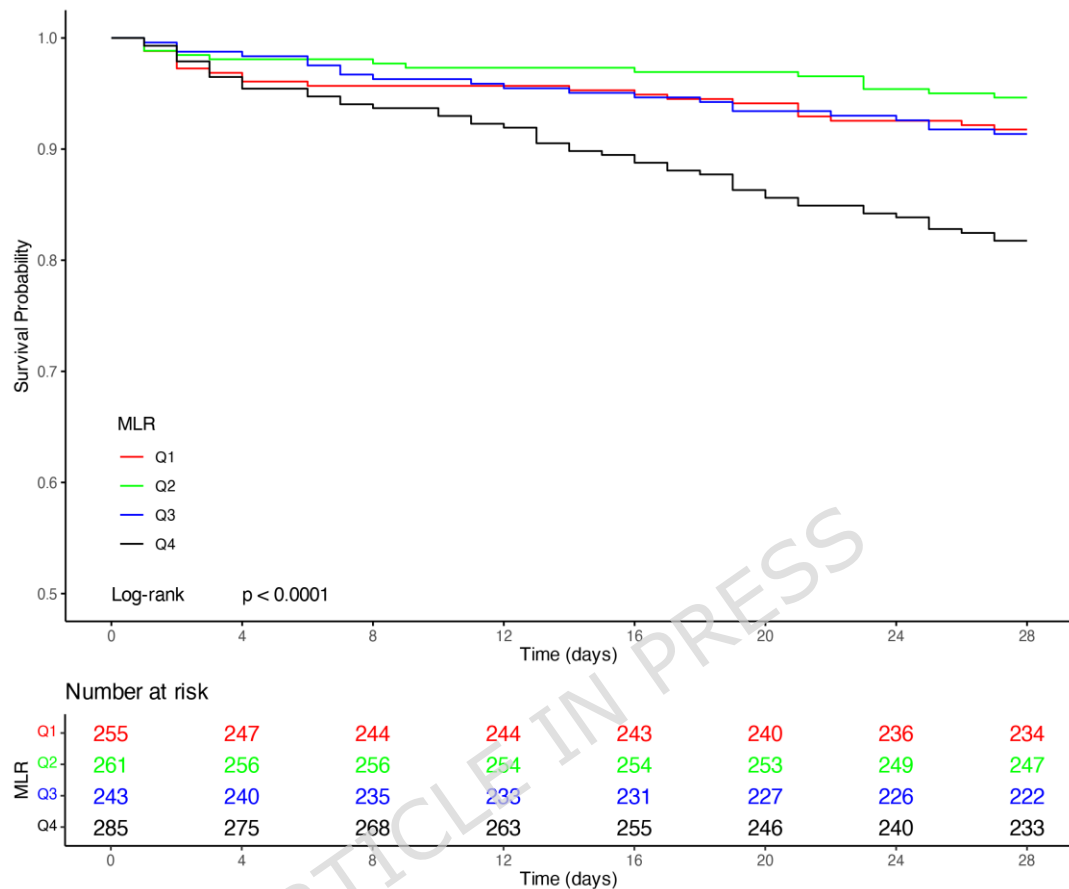


Fig 3. RCS analysis of 28-day (A) and 365-day (B) all-cause mortality after adjusting the covariates. Adjusted covariates: age, hypertension, myocardial infarct, congestive heart failure, cerebrovascular disease, chronic pulmonary disease, diabetes, renal disease, malignant cancer, liver disease, sepsis, gender, language, marital status, race

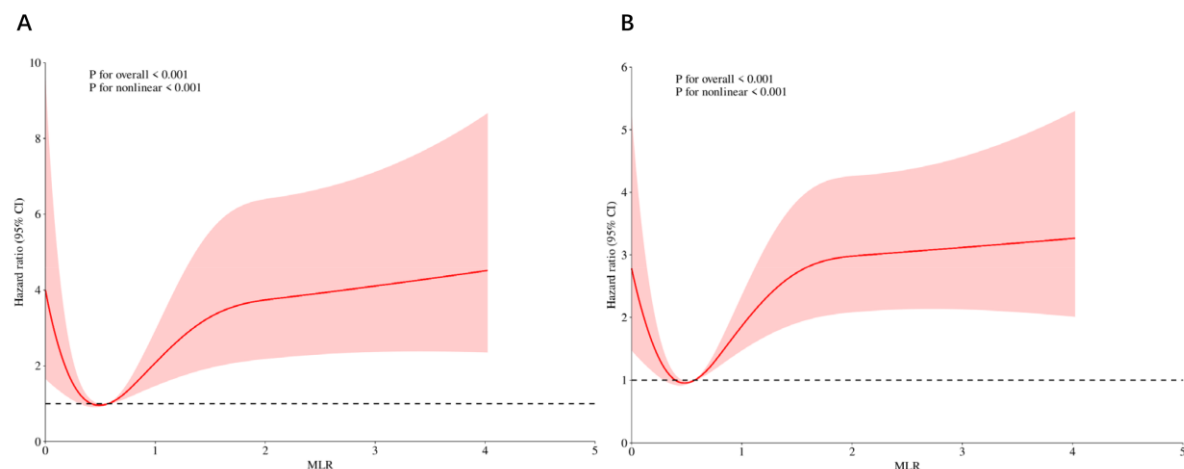


Fig 4. (A) Subgroup forest plot for 28-day all-cause mortality. (B) Subgroup forest plot for 365-day all-cause mortality.

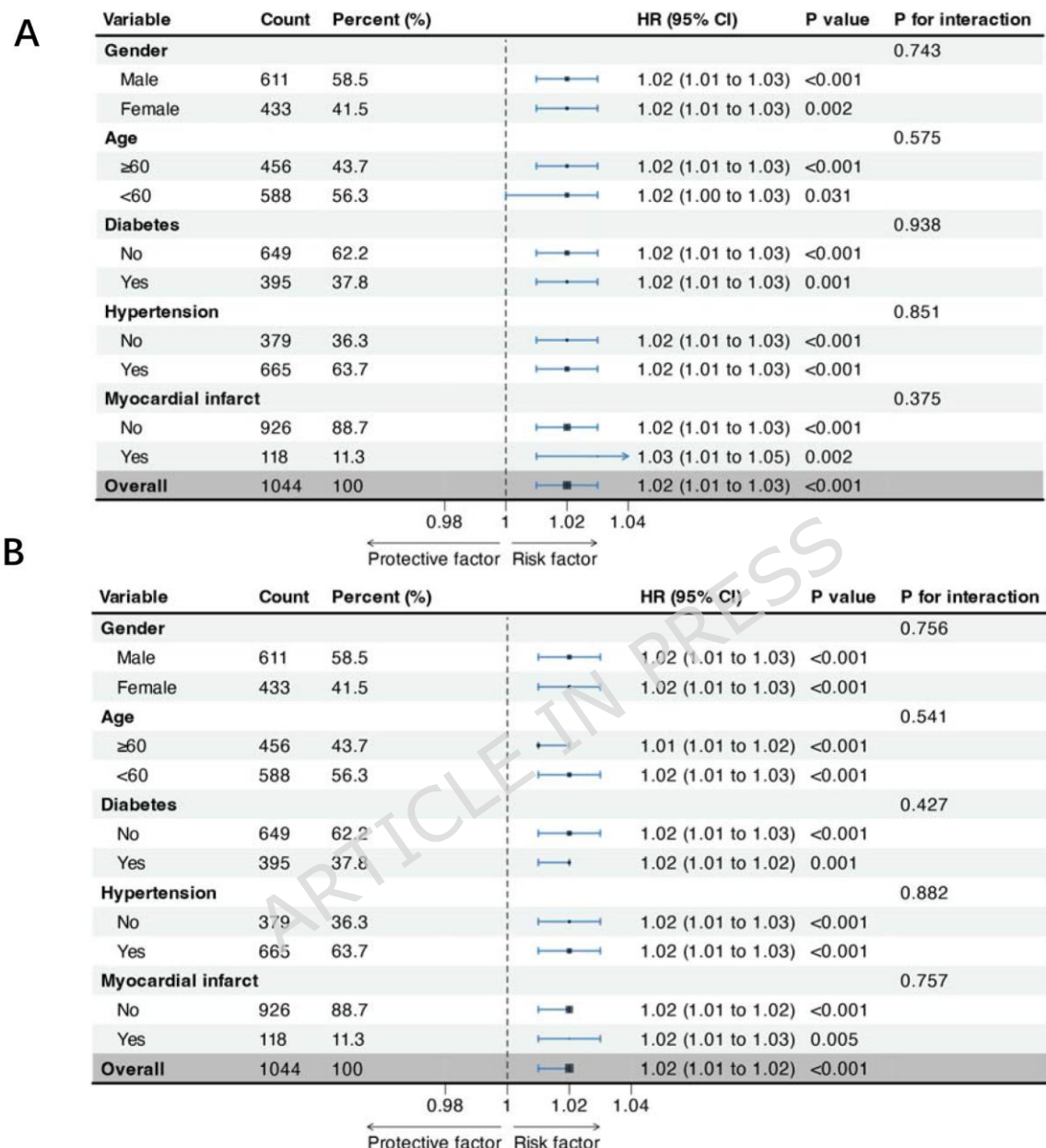


Fig 5. Demographic and clinical feature selection using the least absolute shrinkage and selection operator (LASSO) binary logistic regression model. (A)LASSO coefficient profiles of the 68 texture features; (B) Tuning parameter (λ) selection using LASSO penalized logistic regression with 10-fold cross validation.

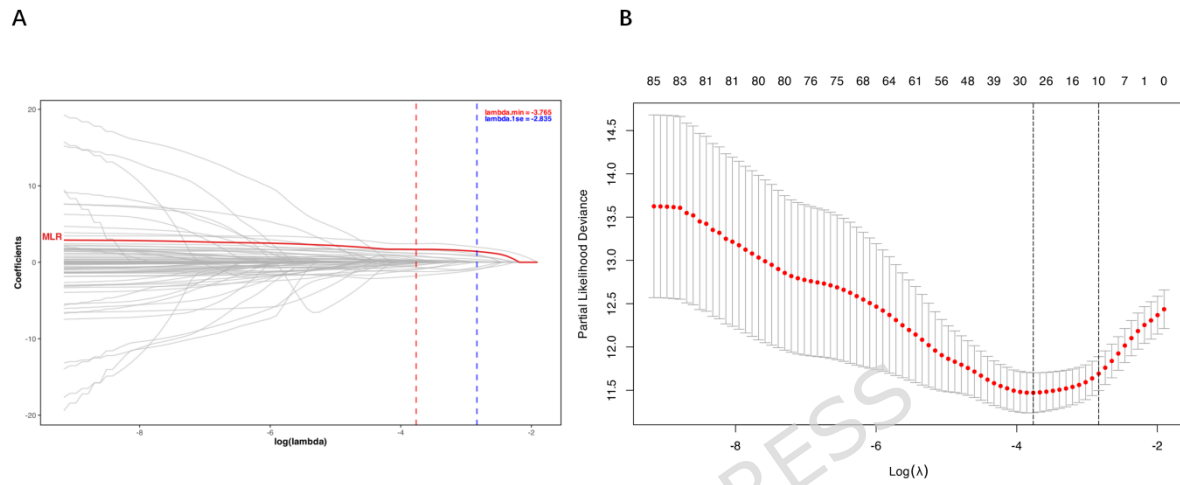


Fig 6. ROC curves of the machine learning algorithms. (A) derivation groups; (B) validation groups.

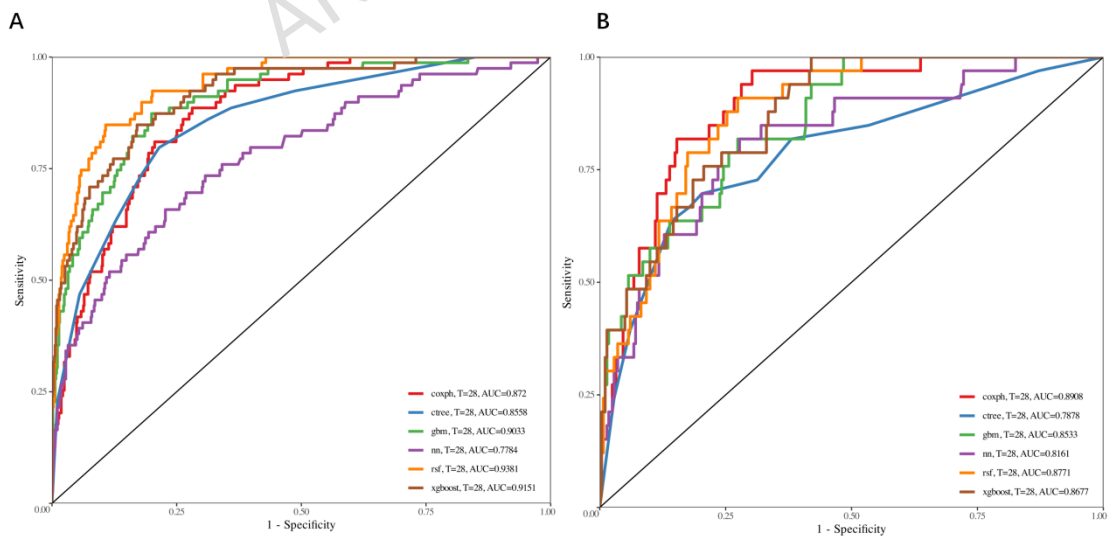


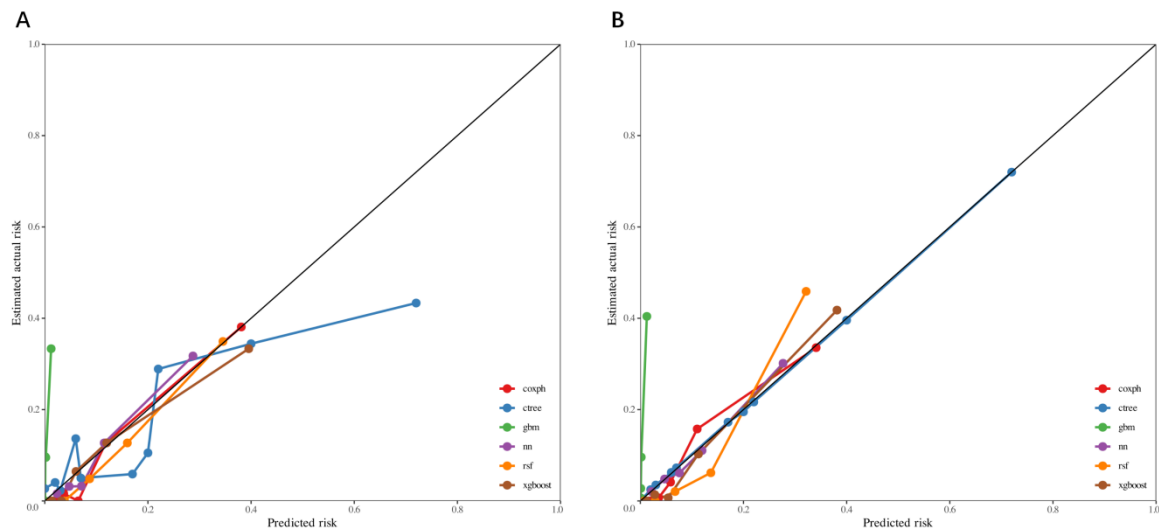
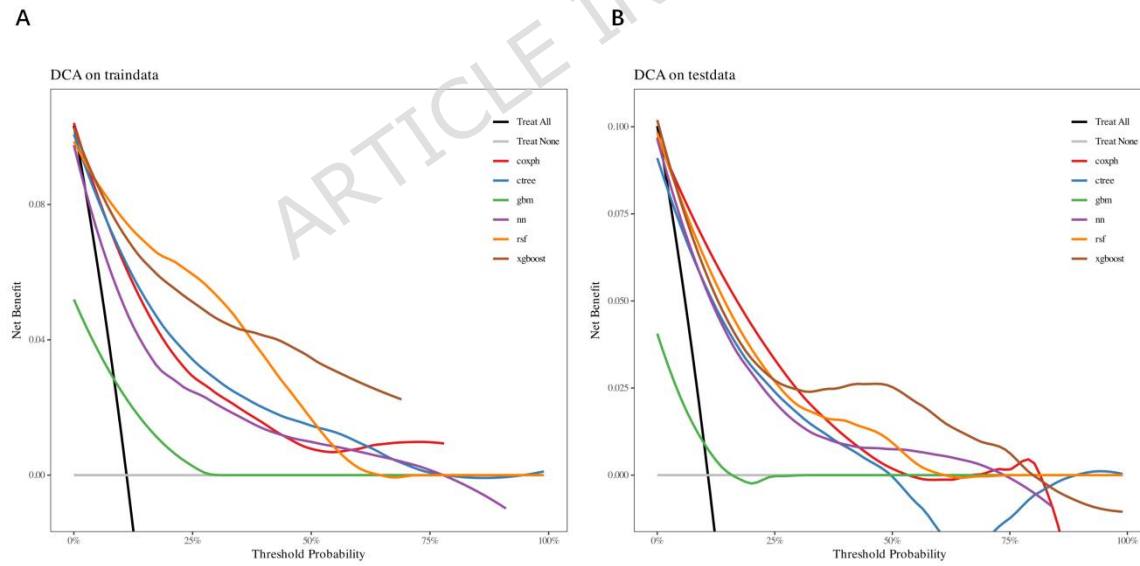
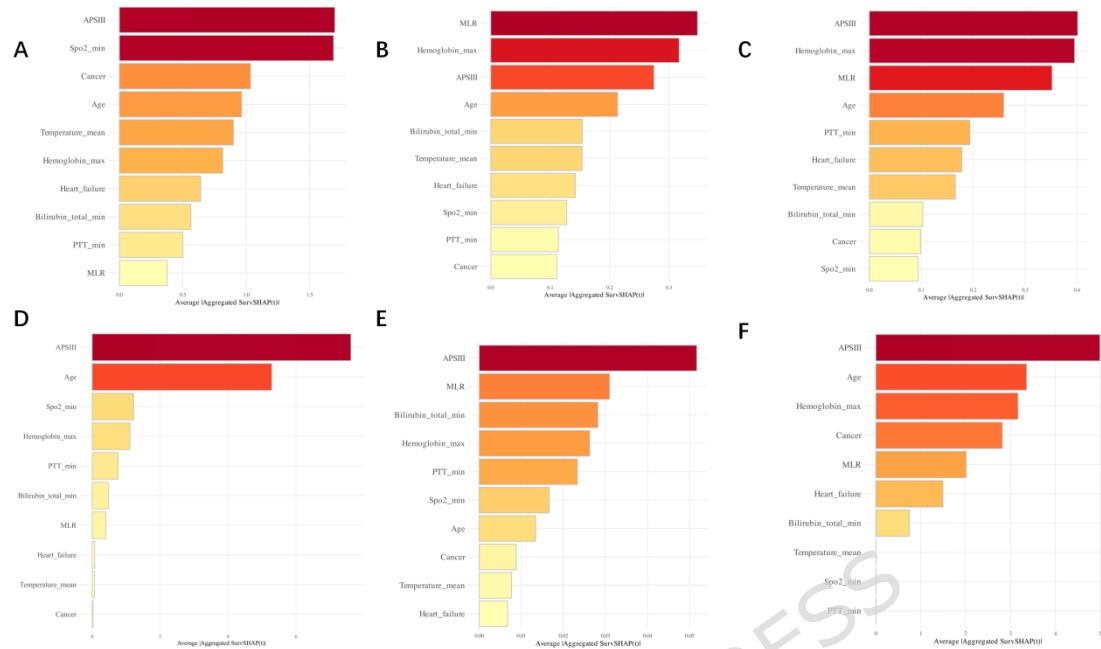
Fig 7. The calibration curve of each model. (A) derivation groups; (B) validation groups.**Fig 8. DCA curves of the machine learning algorithms. (A) derivation groups; (B) validation groups.**

Fig 9. The SHAP summary plots for all models. (A)coxph shap (B)gbm shap (C)xgboost shap (D)nn shap (E)rsf shap (F)cmtree shap



Data Availability Statement

The datasets are available in the physionet (<https://physionet.org/content/mimiciv/0.4/>)

Ethics approval and consent to participate

The MIMIC-IV database was approved by the Massachusetts Institute of Technology (Cambridge, MA) and consent was obtained for the original data collection.

References:

[1] Horibe M, Kayashima A, Ohbe H, Bazerbachi F, Mizukami Y, Iwasaki E, Matsui H, Yasunaga H and Kanai T. Normal saline versus Ringer's solution and critical-illness mortality in acute pancreatitis: a nationwide inpatient database study. *J Intensive Care*, 2024, 12(1):27

[2] Iannuzzi JP, King JA, Leong JH, Quan J, Windsor JW, Tanyingoh D, Coward S, Forbes N, Heitman SJ, Shaheen AA, Swain M, Buie M, Underwood FE and Kaplan GG. Global Incidence of Acute Pancreatitis Is Increasing Over Time: A Systematic Review and Meta-Analysis. *Gastroenterology*, 2022, 162(1):122-134

[3] Szatmary P, Grammatikopoulos T, Cai W, Huang W, Mukherjee R, Halloran C, Beyer G and Sutton R. Acute Pancreatitis: Diagnosis and Treatment. *Drugs*, 2022, 82(12):1251-1276

[4] Glaubitz J, Asgarbeik S, Lange R, Mazloum H, Elsheikh H, Weiss FU and Sendler M. Immune response mechanisms in acute and chronic pancreatitis: strategies for therapeutic intervention. *Front Immunol*, 2023, 14:1279539

[5] Modenbach JM, Moller C, Asgarbeik S, Geist N, Rimkus N, Dorr M, Wolfgramm H, Steil L, Susemihl A, Graf L, Schmoker O, Bottcher D, Hammer E, Glaubitz J, Lammers M, Delcea M, Volker U, Aghdassi AA, Lerch MM, Weiss FU, Bornscheuer UT and Sendler M. Biochemical analyses of cystatin-C dimers and cathepsin-B reveals a trypsin-driven feedback mechanism in acute pancreatitis. *Nat Commun*, 2025, 16(1):1702

[6] Chen F, Xu K, Han Y, Ding J, Ren J, Wang Y, Ma Z and Cao F. Mitochondrial dysfunction in pancreatic acinar cells: mechanisms and therapeutic strategies in acute pancreatitis. *Front Immunol*, 2024, 15:1503087

[7] Swanson K, Wu E, Zhang A, Alizadeh AA and Zou J. From patterns to patients: Advances in clinical machine learning for cancer diagnosis, prognosis, and treatment. *Cell*, 2023, 186(8):1772-1791

[8] Critelli B, Hassan A, Lahooti I, Noh L, Park JS, Tong K, Lahooti A, Matzko N, Adams JN, Liss L, Quion J, Restrepo D, Nikahd M, Culp S, Lacy-Hulbert A, Speake C, Buxbaum J, Bischof J, Yazici C, Evans-Phillips A, Terp S, Weissman A, Conwell D, Hart P, Ramsey M, Krishna S, Han S, Park E, Shah R, Akshintala V, Windsor JA, Mull NK, Papachristou G, Celi LA, Lee P. A systematic review of machine learning-based prognostic models for acute pancreatitis: Towards improving methods and reporting quality. *PLoS Med*. 2025 Feb 24;22(2):e1004432. doi: 10.1371/journal.pmed.1004432. PMID: 39992936; PMCID: PMC11870378.

[9] Wang J, Li H, Luo H, Shi R, Chen S, Hu J, Luo H, Yang P, Cai X, Wang Y, Zeng X and Wang D. Association between serum creatinine to albumin ratio and short- and long-term all-cause mortality in patients with acute pancreatitis admitted to the intensive care unit: a retrospective analysis based on the MIMIC-IV database. *Front Immunol*, 2024, 15:1373371

[10] Djordjevic D, Rondovic G, Surbatovic M, Stanojevic I, Udovicic I, Andjelic T, Zeba S, Milosavljevic S, Stankovic N, Abazovic D, Jevdjic J and Vojvodic D. Neutrophil-to-Lymphocyte Ratio, Monocyte-to-Lymphocyte Ratio, Platelet-to-Lymphocyte Ratio, and Mean Platelet Volume-to-Platelet Count Ratio as Biomarkers in Critically Ill and Injured Patients: Which Ratio to Choose to Predict Outcome and Nature of Bacteremia? *Mediators Inflamm*, 2018, 2018:3758068

[11] Chen X, Lin Z, Chen Y and Lin C. C-reactive protein/lymphocyte ratio as a prognostic biomarker in acute pancreatitis: a cross-sectional study assessing disease severity. *Int J Surg*, 2024, 110(6):3223-3229

[12] Cheng YW, Kuo CH, Kuo YH, Tu TH, Chen YY, Hsu YH and Liao WC. Predictive value of hematologic indices on weaning from mechanical ventilation and 30-day mortality in patients with traumatic brain injury in an intensive care unit: A retrospective analysis of MIMIC-IV data. *Neurotherapeutics*, 2025:e00559

[13] Rees CA, Pineros DB, Amour M, Munseri P, Said J, Magohe A, Matee M, Pallangyo K and von Reyn CF. The potential of CBC-derived ratios (monocyte-to-lymphocyte, neutrophil-to-lymphocyte, and platelet-to-lymphocyte) to predict or diagnose incident TB infection in Tanzanian adolescents. *BMC Infect Dis*, 2020, 20(1):609

[14]Xiang J, Zhou L, Li X, Bao W, Chen T, Xi X, He Y and Wan X. Preoperative Monocyte-to-Lymphocyte Ratio in Peripheral Blood Predicts Stages, Metastasis, and Histological Grades in Patients with Ovarian Cancer. *Transl Oncol*, 2017, 10(1):33-39

[15]Asey B, Pantel TF, Mohme M, Zghaibeh Y, Duhrsen L, Silverbush D, Schuller U, Drexler R and Ricklefs FL. Peripheral blood-derived immune cell counts as prognostic indicators and their relationship with DNA methylation subclasses in glioblastoma patients. *Brain Pathol*, 2025:e13334

[16]Yildirim A, Wei M, Liu Y, Nazha B, Brown JT, Carthon BC, Choi Y, Suh L, Goswamy RV, McClintock GR, Hartman C, Caulfield S, Ciuro J, Goldman JM, Harris WB, Kucuk O, Master VA and Bilen MA. Association of baseline inflammatory biomarkers and clinical outcomes in patients with advanced renal cell carcinoma treated with immune checkpoint inhibitors. *Ther Adv Med Oncol*, 2025, 17:17588359251316243

[17]Song H, Jeong MJ, Cha J, Lee JS, Yoo JG, Song MJ, Kim JH, Lee SJ, Lee HN, Yoon JH, Park DC and Kim SI. Preoperative neutrophil-to-lymphocyte, platelet-to-lymphocyte and monocyte-to-lymphocyte ratio as a prognostic factor in non-endometrioid endometrial cancer. *Int J Med Sci*, 2021, 18(16):3712-3717

[18]Chen X, Cai Q, Deng L, Chen M, Xu M, Chen L, Lin Y, Li Y, Wang Y, Chen H, Liu S, Wu J, Tong X, Fu F and Wang C. Association of inflammatory blood markers and pathological complete response in HER2-positive breast cancer: a retrospective single-center cohort study. *Front Immunol*, 2024, 15:1465862

[19]Yang L, Gao C, Li F, Yang L, Chen J, Guo S, He Y and Guo Q. Monocyte-to-lymphocyte ratio is associated with 28-day mortality in patients with acute respiratory distress syndrome: a retrospective study. *J Intensive Care*, 2021, 9(1):49

[20]Naranbhai V, Kim S, Fletcher H, Cotton MF, Violari A, Mitcheli C, Nachman S, McSherry G, McShane H, Hill AV and Madhi SA. The association between the ratio of monocytes:lymphocytes at age 3 months and risk of tuberculosis (TB) in the first two years of life. *BMC Med*, 2014, 12:120

[21]Cheng YW, Kuo CH, Kuo YH, Tu TH, Chen YY, Hsu YH and Liao WC. Predictive value of hematologic indices on weaning from mechanical ventilation and 30-day mortality in patients with traumatic brain injury in an intensive care unit: A retrospective analysis of MIMIC-IV data. *Neurotherapeutics*, 2025:e00559

[22]Lundberg SM, Erion G, Chen H, DeGrave A, Prutkin JM, Nair B, Katz R, Himmelfarb J, Bansal N and Lee SI. From Local Explanations to Global Understanding with Explainable AI for Trees. *Nat Mach Intell*, 2020, 2(1):56-67

[23]Li X, Tian Y, Li S, Wu H and Wang T. Interpretable prediction of 30-day mortality in patients with acute pancreatitis based on machine learning and SHAP. *BMC Med Inform Decis Mak*, 2024, 24(1):328

[24]Miller J, Wu Y, Safa R, Marusca G, Bhatti S, Ahluwalia G, Dandashi J, Acevedo HG, Farook N, Scott A, Nair V, Adhami A, Dueweke J, Hebbar S and Ekstrom L. Derivation and validation of the ED-SAS score for very early prediction of mortality and morbidity with acute pancreatitis: a retrospective observational study. *BMC Emerg Med*, 2021, 21(1):16

[25]Umans DS, Hoogenboom SA, Sissingh NJ, Lekkerkerker SJ, Verdonk RC and van Hooft JE. Pancreatitis and pancreatic cancer: A case of the chicken or the egg. *World J Gastroenterol*, 2021, 27(23):3148-3157

[26]Gardner TB, Vege SS, Chari ST, Pearson RK, Clain JE, Topazian MD, Levy MJ and Petersen BT. The effect of age on hospital outcomes in severe acute pancreatitis. *Pancreatology*, 2008, 8(3):265-70

[27]Szakacs Z, Gede N, Pecsi D, Izbeki F, Papp M, Kovacs G, Feher E, Dobiszai D, Kui B, Marta K, Konya K, Szabo I, Torok I, Gajdan L, Takacs T, Sarlos P, Godi S, Varga M, Hamvas J, Vincze A, Szentesi A, Parniczky A and Hegyi P. Aging and Comorbidities in Acute Pancreatitis II.: A Cohort-Analysis of 1203 Prospectively Collected Cases. *Front Physiol*, 2018, 9:1776

[28]de Oliveira C, Khatua B, Bag A, El-Kurdi B, Patel K, Mishra V, Navina S and Singh VP. Multimodal Transgastric Local Pancreatic Hypothermia Reduces Severity of Acute Pancreatitis in Rats and Increases Survival. *Gastroenterology*, 2019, 156(3):735-747.e10

[29]Yang Y, Du S, Yuan W, Kou Y and Nie B. Prolonged activated partial thromboplastin time predicts poor short-term prognosis in patients with acute pancreatitis: A retrospective cohort study. *Clin Transl Sci*, 2022, 15(10):2505-2513

Funding

Wei Wu grants from National Natural Science Foundation of China (82302418).

JunYuan Yang grants from Natural Science Foundation of Hubei Province (2024AFB530).

Authors' Contributions

JYY, CTD and MMG contributed equally to this work. WW designed the study, JYY and MMG drafted the manuscript. CTD, SY extracted the data from the MIMIC-IV database. SY, JDC analyzed the data, HDZ, HG, JX and YL guided the literature review. All authors read and approved the final manuscript.

Additional Information

Competing interests

The authors declare no competing interests.

Conflict of interest statement

The authors declare that they have no competing interests.

Acknowledgements

We acknowledged the contributions of the MIMIC-IV 2.2 program registry for creating and updating the MIMIC IV database. Thanks to AJE for polishing the article.

Legends

Fig 1. Screening process for AP patients in ICU and the research process.

Fig 2. 28-day KM survival curve. KM curves showing the survival rates at 28 days for each quartile. MLR: Quartile 1 (<0.32), Quartile 2 ($0.32 \leq \text{MLR} < 0.57$), Quartile 3 ($0.57 \leq \text{MLR} < 1$), and Quartile 4 ($\text{MLR} \geq 1$).

Fig 3. RCS analysis of 28-day (A) and 365-day (B) all-cause mortality after adjusting the covariates. Adjusted covariates: age, hypertension, myocardial infarct, congestive heart failure, cerebrovascular disease, chronic pulmonary disease, diabetes, renal disease, malignant cancer,

liver disease, sepsis, gender, language, marital status, race

Fig 4. (A) Subgroup forest plot for 28-day all-cause mortality. (B) Subgroup forest plot for 365-day all-cause mortality.

Fig 5. Demographic and clinical feature selection using the least absolute shrinkage and selection operator (LASSO) binary logistic regression model. (A) LASSO coefficient profiles of the 68 texture features; (B) Tuning parameter (λ) selection using LASSO penalized logistic regression with 10-fold cross validation.

Fig 6. ROC curves of the machine learning algorithms. (A) derivation groups; (B) validation groups. Coxph, Cox proportional hazards survival learner; GBM, gradient boosting machines; ctree, conditional inference tree; NN, neural network; rsf, Survival Random Forest SRC Learner; xgboost, extreme gradient boosting survival learner; T days; AUC area under the curve.

Fig 7. The calibration curve of each model. (A) derivation groups; (B) validation groups.

Fig 8. DCA curves of the machine learning algorithms. (A) derivation groups; (B) validation groups.

Fig 9. The SHAP summary plots for all models.